

Influence of Nonlinear Effects on the Characteristics of Pulsed High-Power BA DBR Lasers

A. Zeghuzi^{*†}, M. Radziunas[†], A. Klehr^{*}, H.-J. Wünsche^{*†}, H. Wenzel^{*} and A. Knigge^{*}

^{*}Ferdinand-Braun-Institut, Leibniz-Institut für Höchstfrequenztechnik, Gustav-Kirchhoff-Str. 4, 12489 Berlin, Germany.

[†]Weierstrass Institute for Applied Analysis and Stochastics, Mohrenstr. 39, 10117 Berlin, Germany.

[‡]Email: anissa.zeghuzi@fbh-berlin.de

Abstract—We analyze theoretically the influence of nonlinear effects such as spatial holeburning, 2-photon absorption and gain compression on the power-current and beam characteristics of a high-power broad-area distributed Bragg reflector laser with a stripe width of 50 μm operated in pulsed mode. At high injection currents of up to 100 A spatial holeburning, 2-photon absorption and gain compression not only reduce the output power by more than one half but also lead to a shift of the peaks of the lateral near field from the injection stripe center to the edges thus reducing the beam quality.

I. INTRODUCTION

Compact and cost effective light detection and ranging (LIDAR) systems are key components for future automotive and robotic navigation. Due to their small size, low production costs and high efficiency broad-area (BA) diode lasers operated with current pulses in the nanoseconds range are the ideal light sources for these systems. Besides a good beam quality and a high peak power the emission within a narrow spectral range around 905 nm is required. To achieve this the integration of a distributed Bragg reflector (DBR) into the cavity is necessary. Experimentally a strong bending of the power-current characteristics of these lasers at high injection currents is observed. The root cause of this behaviour is theoretically investigated by a numerical solution of the travelling wave equations for the optical field coupled to an effective diffusion equation for the excess carrier density in the active region.

II. MODEL DESCRIPTION

The simulation of the optical field is carried out in the 2-dimensional lateral-longitudinal (x, z)-plane of the active region (Fig. 1). For the simulation of the optical field we use a traveling wave equation for the complex slowly varying amplitudes $u^\pm(x, z, t)$ of the forward and backward traveling optical fields in the longitudinal-lateral plane [1],

$$\frac{1}{v_g} \partial_t u^\pm \pm \partial_z u^\pm = -\frac{i}{2\bar{n}k_0} \partial_x^2 u^\pm - ik_0 \kappa u^\mp - i\Delta\beta u^\pm - \frac{g_r}{2} (u^\pm - p^\pm) + f_{sp}^\pm, \quad (1)$$

where v_g is the group velocity, \bar{n} the real valued reference index, k_0 the free space propagation constant, κ the coupling coefficient of a Bragg grating, f_{sp}^\pm the spontaneous emission factor and $\Delta\beta$ the relative effective propagation factor (projected onto the vertical mode), $\Delta\beta = k_0 \Delta n_N + i \frac{g-\alpha}{2}$

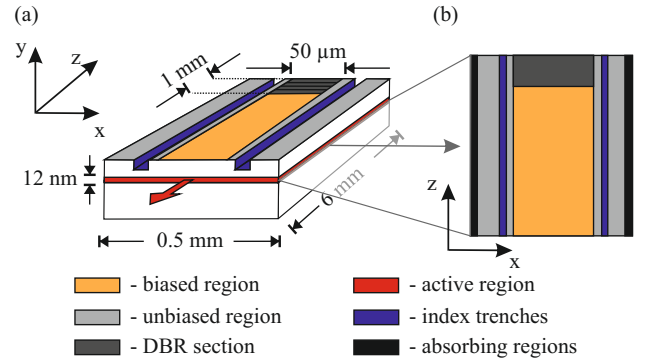


Fig. 1. Schematic representation of the (a) simulated BA DBR laser and (b) the longitudinal-lateral (x, z) plane of simulation.

with $\Delta n_N = -\sqrt{n'_N N}$, where n'_N is the refractive index change factor. For the gain we employ a logarithmic gain model taking into account non-linear gain compression, $g = \frac{g' \ln(\max(N, N_0)/N_{tr})}{1 + \epsilon_g \|u\|^2}$ where $\|u\|^2 = |u^+|^2 + |u^-|^2$ is the local photon density. g' is the differential gain, N_0 the gain clamping carrier density, N_{tr} the transparency carrier density, ϵ_g the gain compression factor and $\alpha = \alpha_0 + \alpha_N + \alpha_{2P}$ the absorption. As an extension to the model described in [1] besides background absorption α_0 we also consider free-carrier absorption $\alpha_N = f_N N$ in the active region with $f_N = 2.1 \cdot 10^{-19} \text{ cm}^2$ and 2-photon-absorption $\alpha_{2P} = f_{2P} \|u\|^2$ with $f_{2P} = 1.9 \cdot 10^{-19} \text{ cm}^2$ [2].

The traveling wave equations are coupled to an ordinary differential equation for the complex slowly varying amplitudes of the polarization fields p^\pm , which model the Lorentzian approximation of the material gain dispersion of amplitude g_r , $\partial_t p^\pm = \gamma(u^\pm - p^\pm) + i\delta\omega p^\pm$, where γ is the half width at half maximum and $\delta\omega$ the central frequency. The excess carrier density N in the active region of thickness d fulfills the diffusion equation

$$\partial_t N = \partial_x (D_{\text{eff}} \partial_x N) + \frac{j}{ed} - R - R_{\text{stim}} \quad (2)$$

with the carrier dependent effective diffusion coefficient $D_{\text{eff}}(N) = \sigma_p \partial_N \varphi_F / e$, where $\sigma_p(N)$ is the conductivity and $\varphi_F(N)$ the quasi-Fermi potential, the injection current density $j(N)$, the non-radiative and spontaneous $R(N)$ and stimulated recombination rate $R_{\text{stim}} = v_g \text{Re} \sum_{\nu=\pm} u^{\nu*} [g u^\nu -$

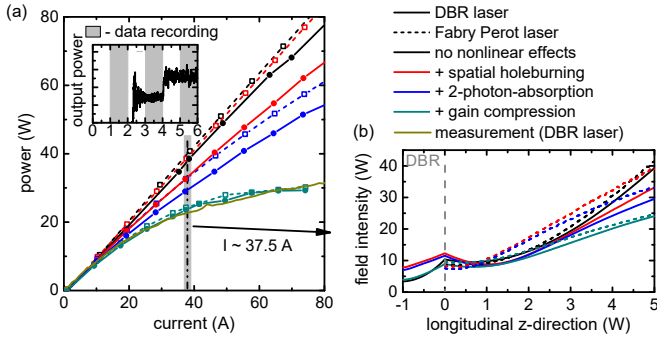


Fig. 2. (a) Power-current characteristics of the DBR (solid curve and bullets) and FP laser (dashed curve and empty squares) without non-linear effects with $r_s = 10^{-6} \Omega\text{cm}^2$ (black), plus spatial holeburning with $r_s = 5.5 \cdot 10^{-5} \Omega\text{cm}^2$ (red), plus 2-photon-absorption (blue) and plus gain compression with $\epsilon_g = 2.5 \cdot 10^{-18} \text{cm}^3$ (cyan). Inset: Start of data recording is 1 ns after applying the corresponding voltage for 1 ns, then the voltage value is changed. Displayed are mean values for that time span. (b) Corresponding longitudinal distributions of the optical power at $I \approx 37.5 \text{ A}$.

$g_r(u^\nu - p^\nu)$. In contrast to the previous model of [1] where a piecewise constant injection current density was assumed, here $j = (U - \varphi_F)/r_s$ below and $j = \partial_x^2 \varphi_F / \Omega$ beside the contact stripe are taken [3]. These are the approximate solutions of the Laplace equation for the quasi-Fermi potential for the holes in the p-doped region where r_s is the series resistance related to the contact area and Ω the sheet resistivity.

III. RESULTS

In what follows we consider two lasers: a 6 mm long DBR laser with a 5 mm long gain section and a 5 mm long Fabry-Pérot (FP) laser both having a $50 \mu\text{m}$ wide contact stripe bounded by $5 \mu\text{m}$ wide trenches for lateral optical and current confinement. The reflectivity of the front facets of both the FP and DBR lasers is $R_f = 0.01$, whereas the reflectivity of the rear facet of the FP laser is $R_r = 0.6$ and of the DBR laser $R_r = 0$. The coupling coefficient of the Bragg grating is $\kappa = 10 \text{cm}^{-1}$, which corresponds to a reflectivity of $R_{\text{DBR}} \approx 0.6$ when lateral waveguide effects are neglected. For the calculation of the power-current (P-I) characteristics shown in Fig. 2(a) the voltage U is tuned from 1.4 V to 3.4 V in 0.2 V steps. The simulation time for each bias is 2 ns. All displayed data give the time averages over the last 1 ns. In Fig. 2(a) the simulated P-I characteristics of the DBR and FP lasers are shown as solid and dashed lines, respectively. For comparison the measured P-I characteristic of a DBR laser with the same design (Fig. 1(a)), operated by 10 ns long current pulses with a repetition frequency of 10 kHz, is also shown. When all nonlinear effects are omitted the slope efficiency of DBR and FP laser are nearly equivalent. As nonlinear effects are subsequently included the slope efficiency is decreased which affects the DBR and BA laser differently. On the one hand spatial holeburning has a bigger effect on the DBR laser. On the other hand due to a larger longitudinal variation of the power within the cavity of the FP laser compared to the DBR laser (Fig. 2(b)), 2-photon-absorption and nonlinear gain compression have a bigger effect on the FP laser. As

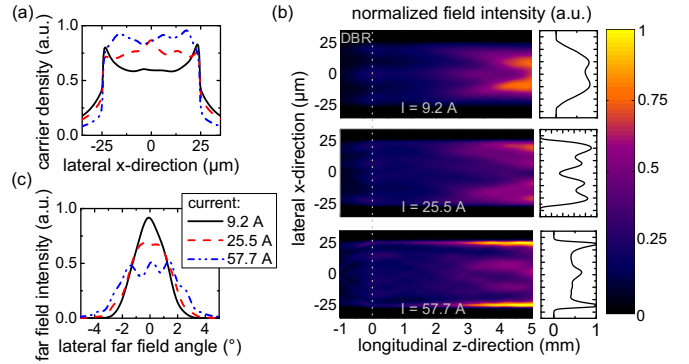


Fig. 3. Simulation results of normalized time-averaged distributions of the (a) carrier density, (b) field intensity within the cavity and near field intensity at the front facet and (c) far field intensity of the DBR laser at $I = 9.2, 25.5$ and 57.7 A .

a result when all nonlinear effects are accounted for, the P-I curves of the FP and DBR laser are almost identical and reproduce the measured P-I curve of the DBR laser if a gain compression factor of $\epsilon_g = 2.5 \cdot 10^{-18} \text{cm}^3$ is assumed. The vertical epitaxial structure is optimized for a reduced minority carrier accumulation outside of the active region so that vertical leakage currents should have only a minor impact. In Fig. 3(a) the simulated time averaged normalized carrier density profile at the front facet is displayed (all effects turned on). At moderate injection currents of around 10 A a carrier accumulation at the stripe edges is visible. It disappears with rising current accompanied by a shift of the peaks of the near field intensity from the center of the stripe to the edges (Fig. 3(b)). As a consequence a widening of the far field distribution (Fig. 3(c)) is observed.

IV. CONCLUSION

At high injection currents nonlinear effects have a major influence on the P-I characteristics of pulsed high-power DBR lasers and reduce the output power at $\approx 70 \text{ A}$ by one half. Due to a larger longitudinal variation of the optical intensity within the cavity a comparable FP laser is more affected by 2-photon absorption and gain compression, whereas spatial holeburning has a bigger impact on the DBR laser. At rising injection currents, the maxima of the carrier density distribution and near field intensity shift from the stripe edges to the centre and from the stripe centre to the edges, respectively. A widening of the far field is visible.

V. ACKNOWLEDGMENT

This work was supported by the German Federal Ministry of Education and Research contract 13N14026 as part of the EffiLAS/PLuS project.

REFERENCES

- [1] M. Radziunas and R. Ciegis. *Mathematical Modelling and Analysis*, 19(5):627–646, 2014.
- [2] M. Sheik-Bahae and E. W. Van Stryland. volume 58 of *Semiconductor and Semimetals*, pages 257–318. Elsevier, Amsterdam, 1998.
- [3] W. B. Joyce. *Journal of Applied Physics*, 53(11):7235–7239, 1982.